



# Portable Hybrid System for Producing Green Hydrogen by Electrolysis Using Energy Generated Through an Archimedean Screw

E. Aliaga Villanueva<sup>†</sup>, P. D. Inga Canales, M. G. Mori Paccori, J. V. Cornejo Tueros and K. G. Ibarra Hinostroza

Environmental Engineering Department, Continental University, Huancayo, Peru

<sup>†</sup>Corresponding author: E. Aliaga Villanueva; 70346388@continental.edu.pe

**Abbreviation:** Nat. Env. & Poll. Technol.

**Website:** [www.neptjournal.com](http://www.neptjournal.com)

*Received:* 23-04-2024

*Revised:* 25-05-2024

*Accepted:* 02-06-2024

## Key Words:

Green hydrogen  
Electrolysis  
Climate change  
Renewable energy  
Hydrogen fuel

## Citation for the Paper:

Aliaga Villanueva, E., Inga Canales, P.D., Mori Paccori, M.G., Cornejo Tueros, J.V. and Ibarra Hinostroza, K.G., 2025. Portable hybrid system for producing green hydrogen by electrolysis using energy generated through an Archimedean screw. *Nature Environment and Pollution Technology*, 24(2), p.D1658. <https://doi.org/10.46488/NEPT.2025.v24i02.D1658>

*Note:* From year 2025, the journal uses Article ID instead of page numbers in citation of the published articles.

## ABSTRACT

At a global level, energy production is predominantly based on the use of conventional resources such as oil, coal, and gasoline; this dependence has led to adverse effects such as climate change and detrimental impacts on human health; consequently, green hydrogen emerges as a renewable energy source. This work develops and analyses the parameters of a portable hybrid system to produce green hydrogen on a small scale in a more efficient way, allowing it to be placed in rural areas to be used as an ecological fuel source. The hybrid system is divided into two stages; for energy production, a microhydraulic system was developed based on an Archimedes screw turbine, which is made up of a mechanical and electrical design, where the electricity produced is stored in a continuous energy source, which supplies the electric current to the electrodes in the alkaline electrolysis process; where a reaction occurs in the water resource to produce green hydrogen and oxygen. It was demonstrated that the turbine, when presenting a greater wetted area and slope of fall, produces a higher electrical potential, while in the electrolysis process to produce green hydrogen and oxygen, it was determined that the appropriate electrolyte to use is potassium hydroxide at 20% because it has greater electrical conductivity unlike sodium chloride and sodium hydroxide; evidencing the most efficient parameters to implement the hybrid system in rural areas to replace the conventional fuel that is used in cooking food.

## INTRODUCTION

Population growth, the continuous development of the global economy, and the persistent search for better living conditions have led to an increase in the energy demand. Energy production is mainly based on the use of conventional resources such as oil, diesel, coal, natural gas, and gasoline, which currently account for 80% of the world's energy demand (Muhsen et al. 2023). This dependence on non-renewable resources has led to adverse effects such as climate change; according to various reports by the Intergovernmental Panel on Climate Change (IPCC), this is caused by greenhouse gas emissions released into the atmosphere by anthropogenic activities, negatively impacting human health and the environment (Bideau et al. 2020). One of the sources for generating electricity in 2021 was the burning of coal, with more than 15 million tonnes of carbon dioxide (CO<sub>2</sub>) emissions into the atmosphere, making it essential to redesign energy strategies towards more sustainable options (Fathi et al. 2023). Emphasis is placed on liquefied petroleum gas (LPG), as it is the most widely used fuel globally as a means of cooking food, where incomplete combustion can generate carbon monoxide (CO) in enclosed spaces without adequate ventilation. This leads to severe household air pollution, directly linked to health risks. According to a recent WHO report, approximately 3.2 million people died prematurely in 2020 due to diseases related to household air pollution (Chen et al. 2023).



*Copyright:* © 2025 by the authors

*Licensee:* Technoscience Publications

This article is an open access article distributed under the terms and conditions of the Creative Commons Attribution (CC BY) license (<https://creativecommons.org/licenses/by/4.0/>).

Consequently, a decisive transition from fossil fuels to renewable and clean energy sources is imperative to improve the efficiency of energy production (Gavrailov & Boycheva 2023). Green hydrogen emerges as a promising energy resource for the future, notable for its high calorific value in combustion. It is a pure, renewable, environmentally friendly, and sustainable energy source with the ability to be stored and transported efficiently (Hassan et al. 2023). According to the International Energy Agency (IEA) projections in the report on the role of hydrogen technologies in ensuring zero carbon dioxide emissions by 2050, it mentions that low-carbon hydrogen will include 62% green hydrogen (Elgarahy et al. 2022). The primary purpose of green hydrogen as a clean energy source is to address the energy crisis and environmental challenges as it has the advantage of having a higher density, being twice as high as other fossil fuels (Niroula et al. 2023). The maximum calorific value of hydrogen at a temperature of 298 K is  $141.8 \text{ MJ.kg}^{-1}$ , while its minimum calorific value is  $120 \text{ MJ.kg}^{-1}$  at the same temperature. These figures indicate a significant increase compared to conventional fuels, such as gasoline, whose value is  $44 \text{ MJ.kg}^{-1}$  at 298 K. This phenomenon underlines the high energy efficiency of hydrogen as one of its main characteristics to be considered (Osman et al. 2022, Yakubson 2022).

Alkaline electrolysis is powered by renewable energies such as wind, solar, and hydropower. These energy sources generate little or no release of greenhouse gases, contributing to the energy industry (Zhang et al. 2024). Hydrogen production by traditional water electrolysis involves the electrolytic decomposition of water into hydrogen ( $\text{H}_2$ ) and oxygen ( $\text{O}_2$ ), using electricity that is generated from renewable sources, producing an ion exchange through an electrolyte (Song et al. 2023).

Alkaline electrolysis produces clean, pure green hydrogen, offering a promising solution to growing global energy demand and reducing greenhouse gas emissions. It is an endothermic process where water vapor, the most abundant greenhouse gas in the atmosphere, is generated as a by-product. Unlike anthropogenic greenhouse gases such as carbon dioxide ( $\text{CO}_2$ ), methane ( $\text{CH}_4$ ), and nitrous oxide ( $\text{N}_2\text{O}$ ), the water vapor released in this process is controlled by the hydrological cycle, providing a more sustainable alternative (Fersch et al. 2022, Muñoz-Maldonado et al. 2023). The advancement and development of electrolysis technologies for green hydrogen production will lead to an increase in the market, reducing the cost of production, which is of utmost importance to improve the cost-effectiveness and efficiency of energy production (Marouani et al. 2023).

Among the research carried out recently, we are told about the production of green hydrogen using renewable

energies. One of the articles entitled “A review of water electrolysis-based systems for hydrogen production using hybrid, solar, wind and hybrid energy systems” (Nasser et al. 2022) stands out among the research. A review of hydrogen production systems was developed using clean energy sources such as solar and wind and the use of an alkaline electrolysis system for the separation of oxygen ( $\text{O}_2$ ) and hydrogen ( $\text{H}_2$ ) under electricity using an electrifier that is combined with renewable energy. As a result, it was found that hydrogen production is a clean energy source that can be stored and transported, which indicates the replacement of fossil fuels. Consequently, it seeks to compete in the global market with an efficient green hydrogen production system.

Another research project is the “Hydrogen production system by alkaline water electrolysis adapted to fast fluctuating photovoltaic energy” (Cao et al. 2023). This electrolysis system is an effective method for hydrogen production due to its long lifetime and high efficiency. It was based on finding a hydrogen production system that is made up of a set of elements, such as a photovoltaic panel, a continuous power source, and an alkaline electrolyzer, together with control and energy management strategies. As a result, a positive efficiency was obtained, based on the fact that the electrolyzer experienced minimal fluctuations that varied every 5 minutes, where the battery operated within the established range.

In contrast to previous research, the present research work focused on producing green hydrogen on a small scale using a hybrid system that can be transported from one place to another. This device is divided into two stages; the construction of an electrolytic cell that has separator plates to separate the production of green hydrogen and gaseous oxygen, as well as electrodes based on AISI 316 stainless steel and a microhydraulic power generation system based on an Archimedes screw that harnesses the kinetic and potential energy of water as a clean and sustainable alternative source. The objective was to demonstrate the most optimal parameters of the portable hybrid system developed for installation in bodies of water and to produce green hydrogen on a small scale, with the purpose of being used to replace conventional fuels used in homes, contributing to the decarbonization of the environment and the health of the inhabitants.

It is envisaged that this system can be used to produce green hydrogen in rural areas with limited hydraulic potential due to its design to take advantage of modest water flows; green hydrogen is intended to be used as an environmentally friendly fuel to replace conventional fuel such as LPG, which is the most commonly used fuel for cooking food in rural areas. In addition, it is envisaged that this research work could

support further research and thus lead to the development of a fully sustainable system.

## MATERIALS AND METHODS

This section presents the two phases that make up the portable hybrid system and is divided into:

1. Micro-hydraulic system
2. Electrolysis

### Micro-Hydraulic System

**Mechanical design:** The design was based on an Archimedes screw turbine, which was divided into two assembled sections. The inner section is comprised of a central body, which was constructed from a 4" PVC pipe; two opposing blades with two revolutions were placed around it along the 83 cm long central body. The central body has no solid filler and the whole section has a thickness of 0.2 cm (Fig. 1). The side ends have a 3/8" hole for inserting and fixing the 100 cm long metal threaded shaft.

To determine the internal geometry, its main variables were considered, such as the outer radius of the blades and the shaft, the diameter, the pitch between blades, and the length of the blades (Dragomirescu 2021), taking into account that the location for the respective tests was a river. The turbine characteristics are specified in Table 1.

The external section was designed based on a 1" square metal profile, and to determine the geometry of the support structure (see Fig. 2a), the size of the auxiliary supports was taken into account to avoid friction between the threaded shaft and the bearing; additionally, a maintenance measure was implemented, which consists of keeping the bearings lubricated to maintain the efficiency of the prototype

Table 1: Characteristics of the Archimedes screw turbine.

Property	Value
Material	PVC
Blade length [cm]	80.00
Central body diameter [cm]	10.16
Outside diameter of blade [cm]	24.20
Pitch between blades [cm]	30.00

(Sánchez et al. 2023). The structure also serves as a support to hold the electrical system and the bases made of 0.5 cm thick acrylic; two lateral bases (see Fig. 2b) and three semicircular bases (see Fig. 2c) that hold the circulation channel (see Fig. 2d), which is where the water circulates and is made of flexible PVC.

To fix the bearings, two 25 cm long auxiliary supports were used (Fig. 3), which served as supports for the internal section; these auxiliary supports were assembled to the metal structure.

For the 3D model (Fig. 4), SolidWorks was used as the design software. In the upper part of the structure, a wooden platform can be visualized to support the electrical system, which is composed of an electrical generator and a current switch, which, using an electrical connection, stores the electricity generated by the micro-hydraulic system in a continuous energy source. The lower part of the structure shows the sections assembled using 3/8" bolts and nuts.

**Electrical system:** For the conversion of mechanical energy into electrical energy, a direct current (DC) electrical generator was used, considering two criteria for its choice: the type of application and the theoretical torque produced by the turbine. The type of application refers to the purpose of the generator, which, in this case, a suitable generator was sought to directly feed the electricity produced in a

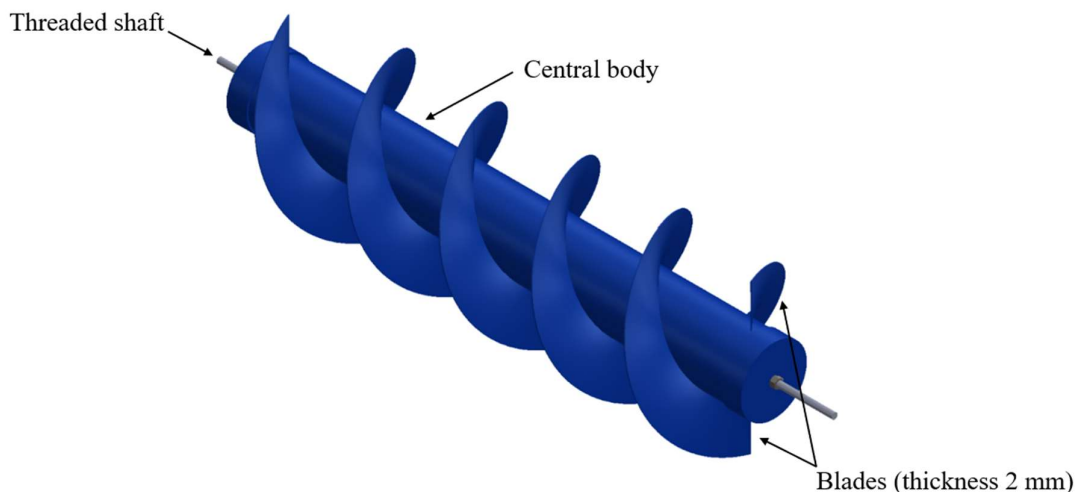


Fig. 1: Archimedes screw turbine.

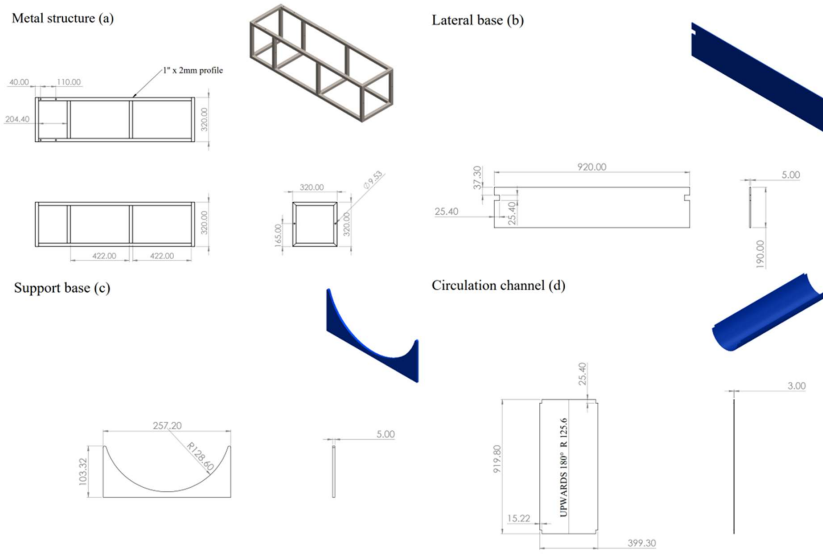


Fig. 2: Diagram of the external section: (a) metal structure; (b) lateral base; (c) support base; (d) circulation channel.

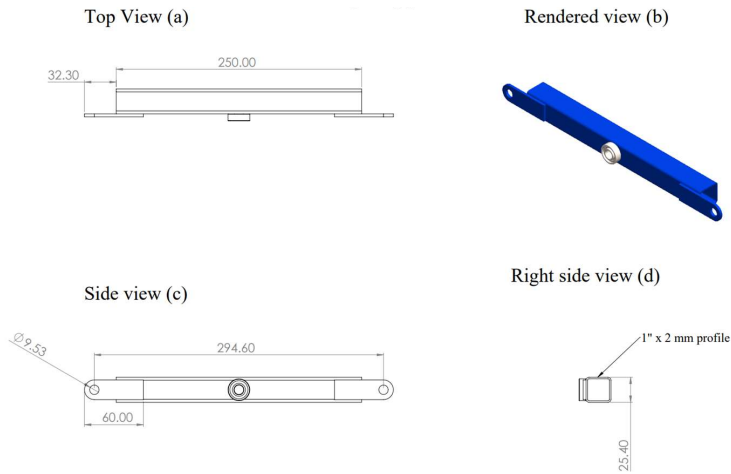


Fig. 3: Auxiliary support.

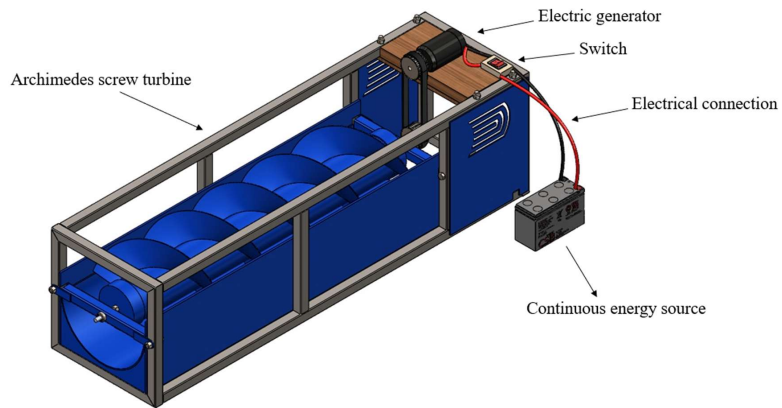


Fig. 4: Rendered design of the micro-hydraulic system with the assembled sections.

continuous energy source, which was used in the laboratory tests to supply electric current to the electrolysis process.

For the torque, equation (1) was used, where the values of height, wetted area, angles, and water are considered; in addition, equation (2) and equation (3) were used to determine the wetted area and inertia  $Y_c$ , respectively (Sánchez et al. 2023):

$$T = \rho \times g \times LT \times Am \times \sin(\theta) \times \tan(\alpha) \times Yc \quad \dots(1)$$

$$Am = 3/8 \times \pi \times Rhe^2 \quad \dots(2)$$

$$Yc = 0.4951 \times Rhe \quad \dots(3)$$

Where,  $T$  is the generated torque in (Nm),  $\rho$  is the density of water ( $1000 \text{ kg.m}^{-3}$ ),  $g$  is gravity ( $9.81 \text{ m.s}^{-2}$ ),  $LT$  is the total length of the turbine in (m),  $Am$  is the wetted area of the water with the turbine blades in ( $\text{m}^2$ ),  $\theta$  is the inclination angle of the turbine in ( $^\circ$ ),  $\alpha$  is the inclination angle of the blades in ( $^\circ$ ),  $Yc$  is the inertia of the blade in (m) and  $Rhe$  is the radius of the blade in (m); assuming 50% wetted area for higher efficiency (Alonso-Martinez et al. 2020).

The calculation was performed considering the criteria of the inner section design, where  $\theta$  and  $\alpha$  were considered  $30^\circ$  and  $40^\circ$  respectively, because the turbine can reach an efficiency of 80%, and these angles have higher efficiency in the turbine (Dragomirescu 2021). By replacing, a torque of 3.79 Nm was obtained. With these two criteria, it was determined to use an electric generator (DC), whose main characteristics are specified in Table 2.

Table 2: Technical specifications of the electrical generator.

Type	DC electric generator with brush
Model	XD-3420
Rated power [W]	30
Rated voltaje [V]	12
Nominal speed [RPM]	3500
Amperage [A]	0.5
Torque [kgfcm]	1

### Electrolysis

**Design of the electrolytic cell:** For the final design of the electrolysis process, an electrolytic cell was constructed, which has the shape of a rectangular prism made of glass and an acrylic lid with a working capacity of approximately  $2900 \text{ cm}^3$  (Fig. 5a) for the production of green hydrogen and oxygen; having a width of 10.5 cm and a length of 23.5 cm. A glass separator plate was used 10 cm away from the sides to separate the anode and cathode to independently produce hydrogen and oxygen. The plate was shorter than the overall height of the cell to allow contact between the anode region and the cathode region; the electrodes had a working depth of 0.5 cm less than the separator plates so that the gases produced did not cross their respective region. Thus, the lower area of the cell was left open for the free circulation of water and the circulation of the current supplied to each electrode (Fig. 5b).

The cell lid had in the middle a circular hole of 1/2" diameter through which the electrolyte solution entered, two

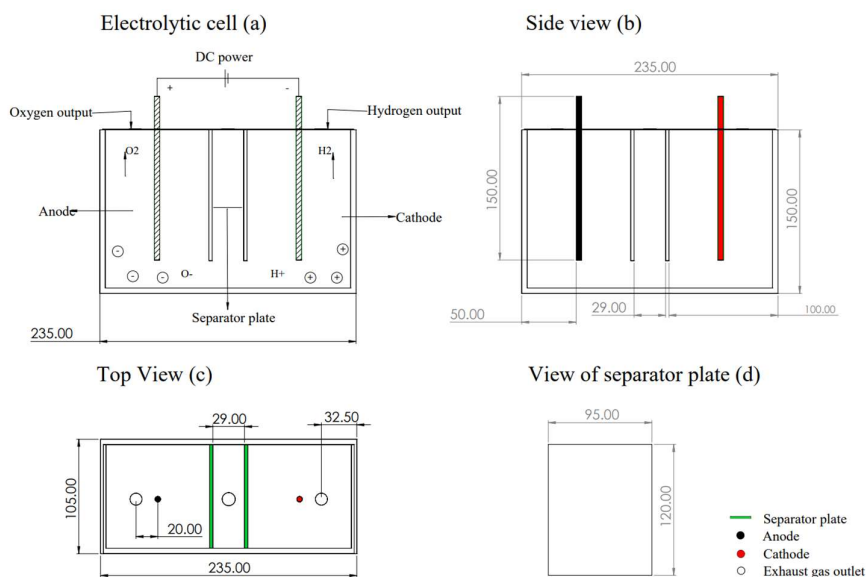


Fig. 5: Schematic of the electrolytic cell: (a) Electrolysis process in the electrolytic cell; (b) Side view of the electrolytic cell; (c) Top view of the electrolytic cell; (d) Separator plate.

circular holes 5 cm from the sides to insert the electrodes, and two other circular holes of 8 mm diameter 3 cm from the sides to insert the valves, which serve as an outlet for the gases from each region (Fig. 5c).

The separator plate was 9.5 cm wide and 12 cm high (Fig. 5d). A space was provided between the plates to insert a 1/2" nipple into the hole in the lid.

**Electrodes:** AISI 316 stainless steel was used for the anode and cathode; it is a non-noble metal. It contains approximately 19% chromium, 12% nickel, and 68.40% iron (Hamidah et al. 2018). The choice of this material is based on its outstanding properties, with an emphasis on its corrosion resistance, which plays a critical role in ensuring the durability and efficiency of the alkaline electrolysis process. During the electrolysis process, the anode and cathode electrodes are connected to a continuous energy source; oxygen is produced on the anode surface, and green hydrogen is generated on the cathode surface (Albornoz et al. 2023). The electrodes are formed by a 1/4" x 15 cm screw, where 13 AISI 316 steel plates are inserted, which have a size of 8 cm x 8 cm giving a wide surface with respect to the electrolytic cell to counteract the presence of gas bubbles that have a negative influence by obstructing the electrolysis process (Babay et al. 2023), in addition, these plates have a perforation in the middle and using 1/4" nuts they are coupled (Fig. 6).

**Electrolyte solution:** To determine the electrolyte solution to be used in our cell, distilled water was used as the main solution, being a pure solution and free of unwanted components, and a comparison was made between three electrolytes: potassium hydroxide (KOH), sodium hydroxide

(NaOH) and sodium chloride (NaCl). The purpose of the electrolytes is to improve the efficiency of the electrolysis process, where characteristics such as corrosion in AISI 316 steel were taken into account. The NaCl presents a higher corrosion rate because the Cl ion makes it highly active for the corrosion process; NaOH and KOH are almost similar because they present the hydroxyl (OH) in their composition, increasing the electrical conductivity of the solution, which is proportional to the corrosion, being KOH the electrolyte with less corrosion (Colli et al. 2019, Hamidah et al. 2018); also a comparison of these electrolytes in different concentrations was made regarding the electrical conductivity they reached, which is presented in the results chapter.

### Simulation of the Portable Hybrid System

The hybrid system has the advantage of mobility by incorporating an Archimedes screw turbine which, due to its attributes, facilitates the disassembly and subsequent reassembly of its components; this characteristic transforms it into a portable device as it does not have a fixed structure like those observed in dams. The electrolytic cell is also portable, and both devices interact synergistically to produce green hydrogen, where the microhydraulic system, for its part, constitutes the device in charge of obtaining energy for the electrolysis process, consolidating itself as a sustainable procedure.

The simulation is shown in Fig. 7 details the value chain of our hybrid system for the production of green hydrogen. Initially, the hybrid system was placed in a useable water resource, such as low-flow rivers or water channels. In the

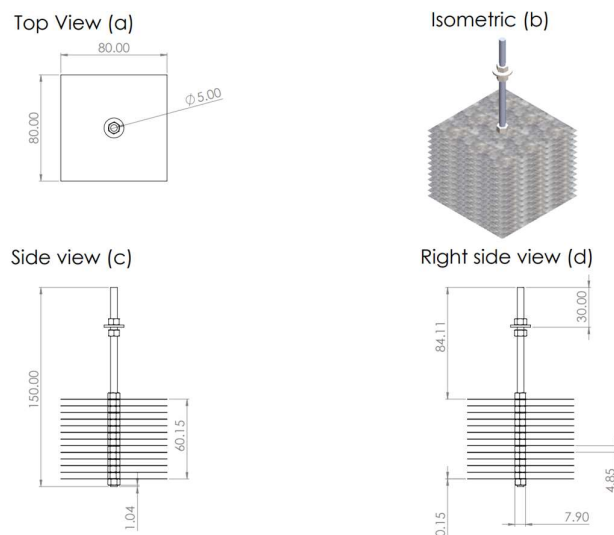


Fig. 6: Electrode.

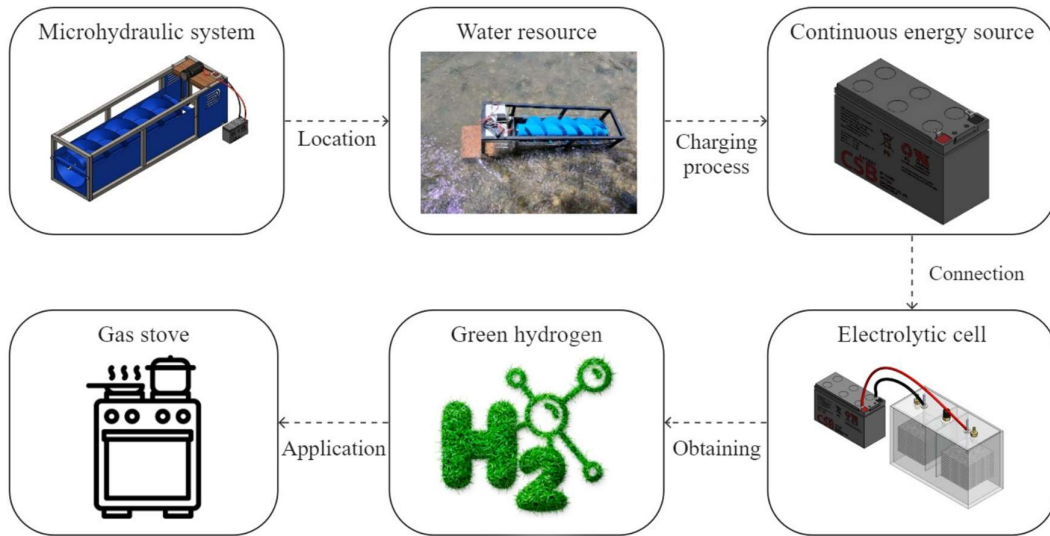


Fig. 7: Green hydrogen value chain.

study carried out, the turbine was placed in a river for the generation and storage of electrical energy. At the end of the charging process of the continuous energy source, this corresponding component is removed from the microhydraulic system and connected to the electrolytic cell using an electrical connection to the electrodes, where the electrolysis process is carried out to obtain the green hydrogen and for its application in stovens, tests were conducted which are detailed in the results section, demonstrating its viability to replace LPG as an ecological fuel for cooking food.

**Experimental Configuration**

**First stage: Performance of the Micro-Hydraulic System**

**Volumetric flow rate:** The volumetric flow rate was determined using the current meter method, where the equipment measures the water velocity at a certain point; first, the width of the channel was calculated to determine the number of cross sections to be divided from the total section. In each section, the flow velocity and depth were calculated using the equipment correctly, taking into consideration that, to measure the flow velocity, the current meter was placed

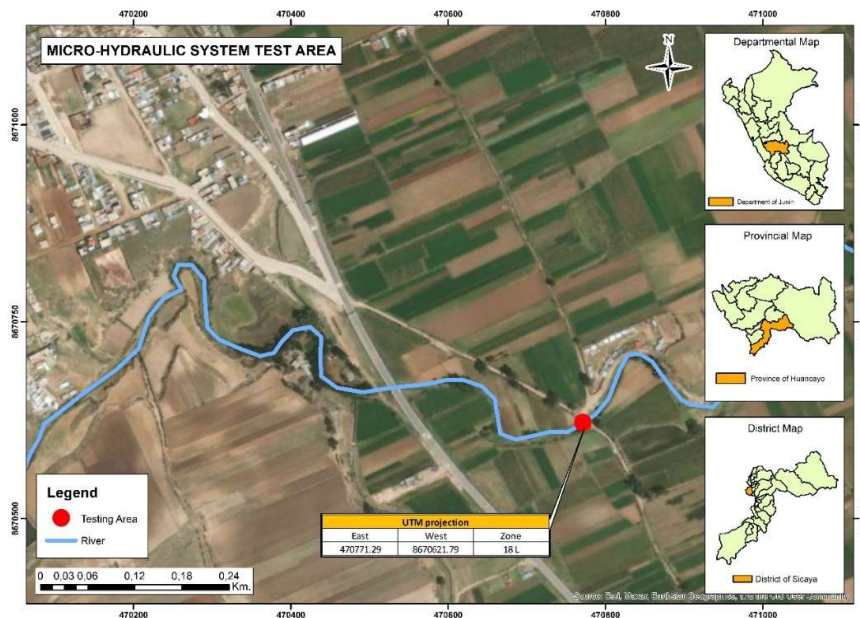


Fig. 8: Micro-hydraulic system test area.

at an intermediate distance from the water depth to avoid obstacles and obtain more representative measurements. Fig. 8 shows the area where the micro-hydraulic system was tested.

**Mechanical potential:** To determine the theoretical potential of the Archimedes screw design, equation (4) was used, which refers to the energy available in the water flowing through the micro-hydraulic system to convert mechanical energy into electrical energy (Sánchez et al. 2023):

$$P_H = T \times w \quad \dots(4)$$

Where  $P_H$  is the theoretical potential in (W),  $T$  is the torque obtained from equation (1) in (Nm), and  $w$  is the angular velocity in (rad/s) which is determined using equation (5):

$$w = \frac{Q \times \tan(\alpha)}{Am \times Yc} \quad \dots(5)$$

Where  $Q$  is the turbine inflow in ( $\text{m}^3 \cdot \text{s}^{-1}$ ),  $\alpha$  is the inclination angle of the blades in ( $^\circ$ ),  $Yc$  is the blade inertia in (m), and  $Am$  is the wetted area of the water with the turbine blades in ( $\text{m}^2$ ).

**Fall slope:** Two level values were determined with respect to the angle of fall; the first level value was equal to the natural slope of the river, where equation (6) was used, representing Manning's formula (Díaz-Salas et al. 2020):

$$n = \frac{1}{Vf} \times Rh^{2/3} \times S^{1/2} \quad \dots(6)$$

Where  $Vf$  is the flow velocity in ( $\text{m} \cdot \text{s}^{-1}$ ),  $Rh$  is the hydraulic radius of the channel in (m), which was determined with equation (7),  $S$  is the slope in (%), and  $n$  is the roughness coefficient, where the value of  $n$  was determined using Cowan's method described in equation (8):

$$Rh = \frac{Ah}{P} \quad \dots(7)$$

$$n = (n0 + n1 + n2 + n3 + n4) \times m5 \quad \dots(8)$$

Where  $Ah$  is the hydraulic area in ( $\text{m}^2$ ), and  $P$  is the perimeter in (m), taking into account that they correspond to the total wetted section (Islam et al. 2022). Table 3 is used to determine the value of each variable of Cowan's method, taking into account the channel conditions observed during the field study.

**Influence of wetted area and fall slope on rotational speed and electric potential:** In the influence tests, the dependent and independent factors were determined, taking into account that the turbine has a fixed design and that it was placed in a river. The independent factors are the fall slope (PC) and the wetted area (Am) with two-level values to study their performance with respect to the electrical potential and to contrast with the rotational speed of the turbine;

Table 3: Criteria and numerical values for the Cowan method (Díaz-Salas et al. 2020).

Channel condition		Values	
Material considered	Land	n0	0.020
	Rock cutting		0.025
	Fine gravel		0.024
	Coarse gravel		0.028
Degree of Irregularity	Soft	n1	0.000
	Minor		0.005
	Moderate		0.010
Cross Section Variation	Severe		0.020
	Gradual	n2	0.000
	Occasionally alternating		0.005
Effect of Obstructions	Frequently alternating		0.010-0.015
	Insignificant	n3	0.000
	Minor		0.010-0.015
Vegetation	Appreciable		0.020-0.030
	Severe		0.040-0.060
	Low	n4	0.005-0.010
Number of Meanders	Medium		0.010-0.025
	High		0.025-0.050
	Very high		0.050-1.000
Number of Meanders	Minor	m5	1.000
	Appreciable		1.150
	Severe		1.300

Table 4: Full factorial design.

Fall slope	Wetted area	Run number
PC 1	Am 1	1
	Am 1	2
PC 2	Am 2	3
	Am 2	4

consequently, a  $2^k$  full factorial design was used, with  $k = 2$  (Table 4).

The river section was selected according to the physical conditions of the terrain in order to be able to manipulate the fall slope and the wetted area. Regarding the level values, it was taken into account that the initial fall slope of the turbine was the same as the natural fall slope of the river, and for the second value, a 14.5 cm high block was placed. For the wetted area, the turbine was placed at different points to have a smaller wetted area and another similar to the ideal, which allowed the four possible combinations of the experimental design to be carried out, considering three repetitions to obtain representative measurements. For data collection, a multimeter (Samwin DT830D) was used, which gave us the value of voltage and current intensity, and a

digital tachometer (CHECK-LINE CDT-1000HD) was used to determine the rotational speed in revolutions per minute (RPM). Using equation (9), the electrical potential of the turbine was determined:

$$Pe = Volt \times Ic \quad \dots(9)$$

Where  $Pe$  is the electric potential in (W),  $Ic$  is the current intensity in (A), and  $Volt$  is the voltage in (V).

**Second stage: To Determine the Amount of Hydrogen Produced by the Electrolytic Cell**

**Electrolyte comparison:** To determine the electrolyte to be dissolved in the distilled water, a comparison was made between seven concentrations of KOH, NaOH, and NaCl with an electrical conductivity test using the combined meter (HANNA HI9828); where the optimum amount of electrolyte to be used was the concentration that achieved the highest electrical conductivity in the solvent.

**Volumetric flow and mass flow of green hydrogen:** This test was based on a one-group design, where the only factor to be evaluated is the production capacity of the electrolytic cell, considering three repetitions since there are fixed factors such as the electrode material, the voltage of the continuous energy source, and the concentration of the electrolyte.

The source that supplied energy to the electrolytic cell was previously obtained from the microhydraulic system. Regarding data collection, the displacement of the water was used to determine the volume of green hydrogen; with a manometer placed in the storage vessel, the gauge pressure of the gas produced was obtained, and the ideal gas law was also used since the green hydrogen produced at environmental pressure (Colli et al. 2019); equation (10) was used to determine the mass of the gas produced, which when interacting with a determined time the mass flow was obtained in ( $g.s^{-1}$ ) as indicated in equation (11) and when interacting time with volume, the volumetric flow of the produced gas was obtained in ( $L.s^{-1}$ ) which is indicated in equation (12):

$$Pabs \times v = \frac{m}{M} \times R \times Tc \quad \dots(10)$$

$$\dot{m} = \frac{m}{t} \quad \dots(11)$$

$$\dot{v} = \frac{v}{t} \quad \dots(12)$$

Where  $Pabs$  is the absolute pressure in (atm) and to determine its value, equation (13) was used;  $v$  is the volume of green hydrogen produced in (L),  $m$  is the mass of the gas in (g),  $M$  is the molar mass of the gas in ( $g.mol^{-1}$ ),  $R$  is the ideal gas constant ( $0.0821 Latm.mol^{-1}.K^{-1}$ ),  $Tc$  is the temperature of the electrolytic cell in (K) which was calculated using a digital pyrometer and  $t$  is the time in (s):

$$Pabs = Pman + Patm. \quad \dots(13)$$

Where  $Pman$  is the gauge pressure in (atm), and  $Patm$  is the atmospheric pressure in (atm), which was determined using equation (14) representing the barometric equation:

$$Patm = P0 \times e^{-\frac{Mm \times g \times h}{R \times Tg}} \quad \dots(14)$$

Where  $P0$  is the pressure at standard level (1 atm),  $Mm$  is the molar mass of air ( $0.02896 kg.mol^{-1}$ ),  $g$  is gravity ( $9.81 m.s^{-2}$ ),  $h$  is the height above sea level in (m),  $R$  is the ideal gas constant ( $8.31432 J.mol^{-1}.K^{-1}$ ), and  $Tg$  is the temperature according to the geographical location in (K).

**RESULTS AND DISCUSSION**

Below are the results of the experimental work in two stages:

**First stage: Performance of the Micro-Hydraulic System**

**Volumetric flow rate:** According to the studies carried out in the selected section of the river, the volumetric flow rate was determined using the current meter method. Table 5 shows the calculated measurements, where the width of the river was determined using a flexometer and divided into four cross sections; in addition, the flow velocity and depth were calculated using a current meter (Global Water FP111) in each established section.

To process the collected data, the HidroEsta software was used as a tool that facilitates and simplifies various calculations, where the data was inserted to calculate the flow rate (Table 6).

According to the processed data, the total flow rate of the section was determined, the value of which is  $0.7118 m^3.s^{-1}$ . In addition, the HidroEsta software gave us the complete geometry of the river, which can be seen in Fig. 9.

Table 5: Data recording of the selected section.

Width [m]	Number of sections	Depth [m]	Flow velocity [ $m.s^{-1}$ ]
4.35	4.00	0.24	0.00
		0.13	0.80
		0.20	1.10
		0.23	1.30
		0.28	0.00

Table 6: Results of each cross-section.

Section	Area [ $m^2$ ]	Average velocity [ $m.s^{-1}$ ]	Volumetric Flow [ $m^3.s^{-1}$ ]
1	0.20	0.40	0.08
2	0.18	0.95	0.17
3	0.23	1.20	0.28
4	0.28	0.65	0.18

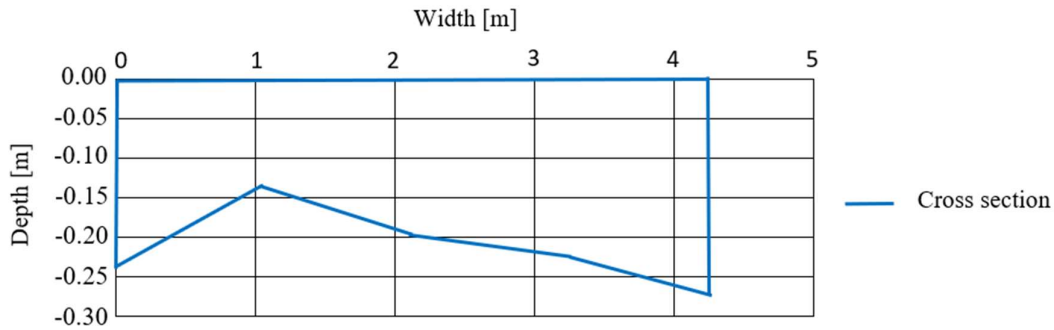


Fig. 9: Complete river geometry.

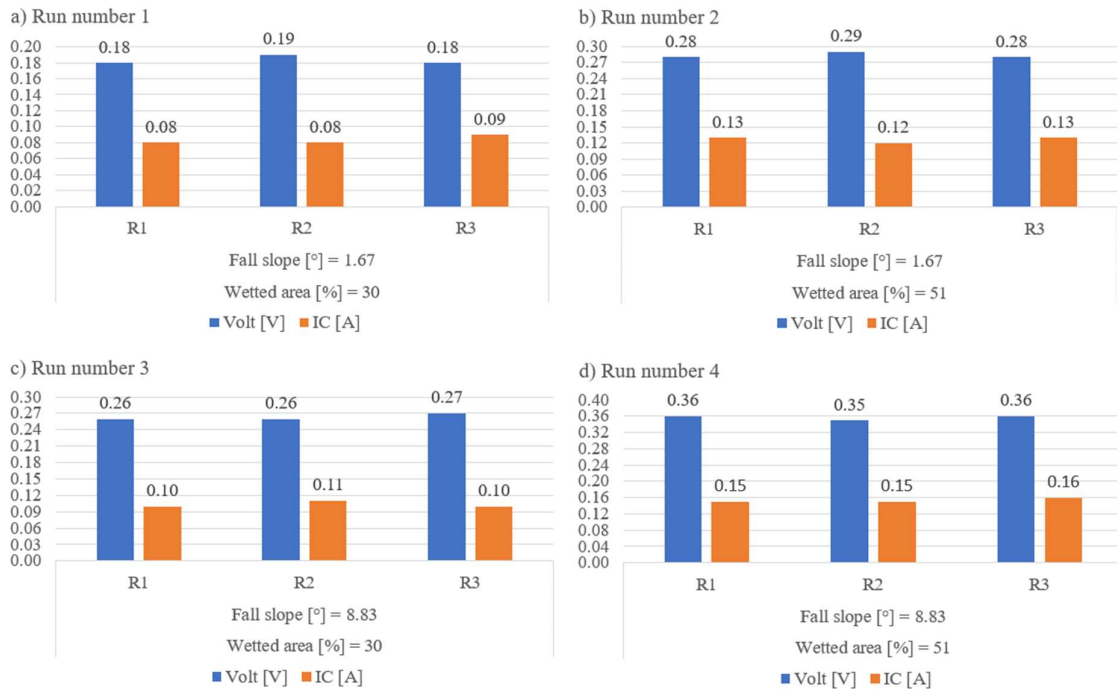


Fig. 10: Voltage and Current Intensity of the micro-hydraulic system.

**Mechanical potential:** Consequently, the theoretical potential of the micro-hydro system was determined using equation (4), where the electrical potential that the turbine can reach is 620.25 W.

**Fall slope:** The characteristics of the channel can be seen in Table 7, where the average flow velocity of the selected section was determined using Table 6, the perimeter and the hydraulic area were determined using Fig. 9, and the hydraulic radius was determined with equation (7), in addition, the Manning's roughness coefficient was determined with equation (8) considering that the values of each variable were determined according to the conditions observed in the channel, and their values are shown in Table 3. With these values, Manning's formula was applied,

giving a slope of 2.91%, which, expressed in degrees, would be  $1.67^\circ$ .

For the second level value, the natural slope of the channel was taken as a reference, which has a value of 2.91%, where every 100 m horizontal rises 2.91 m vertical; expressing

Table 7: Channel characteristics.

Characteristics	Value
Flow velocity [ $\text{m}\cdot\text{s}^{-1}$ ]	0.80
Hydraulic area [ $\text{m}^2$ ]	0.89
Perímetro [m]	9.20
Hydraulic radius [m]	0.10
Manning's roughness Coefficient	0.045

this in the length of the turbine, it was obtained that every 1.1495 m horizontal rise 0.0336 m vertical for a diagonal of 1.15 m, which represents the length of the turbine; with these dimensions a 14.5 cm block was added at the base of the turbine inlet to increase the slope, giving a value of 8.83°.

**Influence of wetted area and fall slope on rotational speed and electric potential:** At this stage, the wetted area is in (%); it was determined according to the contact of the water with the turbine blades, where 50% means that the contact has a height equal to the radius of the blades; a height meter was used in centimeters attached to the inlet base which indicates the height of the water level, then the turbine was placed at two different points and it was determined that there was a wetted area of 30% and 51%.

With the level values determined for each independent variable, field tests were carried out to determine the *Volt* and the *Ic*, as shown in Fig. 10, which are necessary variables in the calculation of the electric potential.

To simulate the interaction between the falling slope and wetted area with rotational speed and electrical potential, Minitab was used as the processing software for the full factorial design, where two interactions were performed, and twelve data were inserted for each interaction, with a p-value significant as it was less than 0.05, thus demonstrating that there is an effect between these factors and the dependent variables. Fig. 11 shows the interaction of the falling slope and wetted area with the rotational speed, where the lowest amount of rotational speed generated by the turbine is 50

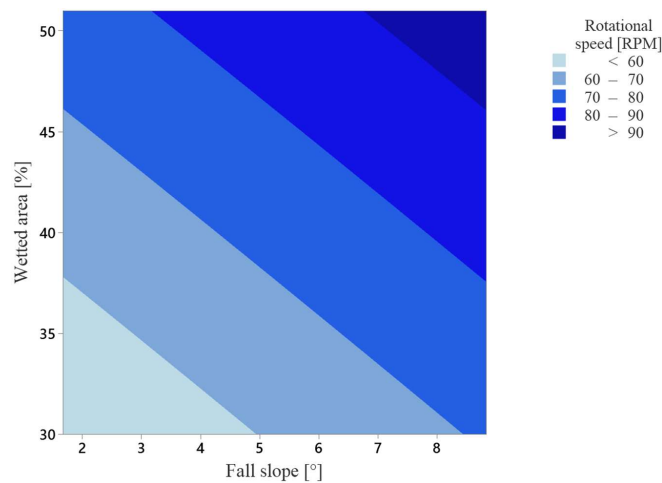


Fig. 11: Contour of rotational speed as a function of fall slope and wetted area.

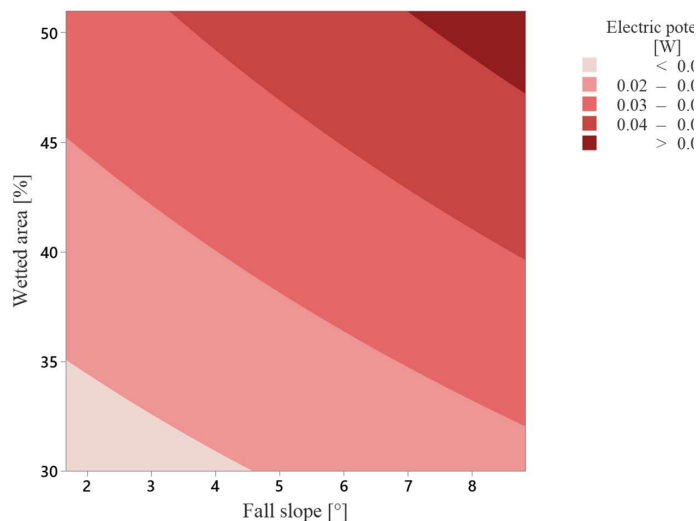


Fig. 12: Contour of the electric potential as a function of fall slope and wetted area.

RPM, which occurs when the slope is  $1.67^\circ$ , and the wetted area is 30%, while 96 RPM is generated when the slope is  $8.83^\circ$ , and the wetted area is 51%, being these the most efficient values of the factors. Consequently, it is established that increasing the fall slope and the wetted area produces a higher rotational speed.

The second interaction represents the effect of the factors with the desired response, which would be the electric potential, where the values of each run were determined using equation (9) with the values in Fig. 10. Fig. 12 shows that the micro-hydraulic system presents a lower electric potential of 0.015 W when the slope is  $1.67^\circ$ , and the wetted area is 30%; while 0.055 W is generated when the slope is  $8.83^\circ$ , and the wetted area is 51%, being these the most efficient values of the factors to generate electricity. It was determined that the micro-hydraulic system is more efficient when there is a higher fall slope and wetted area.

Additionally, a Spearman's Rho test was performed to determine the correlation between the rotational speed and

the electrical potential (Fig. 13). It was determined that the rotational speed represented in Fig. 11 is related to the electrical potential produced by the micro-hydraulic system demonstrating that the higher the RPM, the more electricity is generated.

**Second Stage: To Determine the Amount of Hydrogen Produced By the Electrolytic Cell**

**Electrolyte comparison:** The electrolyte to be used in the solution was determined, where it was found that KOH has a higher electrical conductivity, given that from a concentration of 20%, it exceeds  $400 \text{ mS}\cdot\text{cm}^{-1}$  (Fig. 14), being the highest measurement value allowed by the equipment. In addition, KOH at a concentration of 20% demonstrates greater effectiveness for the alkaline electrolysis process (Cao et al. 2023, Colli et al. 2019), being the suitable concentration that was used to prepare the electrolyte solution, while NaCl has the lowest values of electrical conductivity. The curve of these electrolytes tends to decrease after a certain concentration.

			Electric potential	Rotational speed
Spearman's Rho	Electric potential	Correlation coefficient	1,000	1,000**
		Sig. (bilateral)	.	.
		N	4	4
	Rotational speed	Correlation coefficient	1,000**	1,000
		Sig. (bilateral)	.	.
		N	4	4

Fig. 13: Correlation analysis between rotational speed and electric potential.

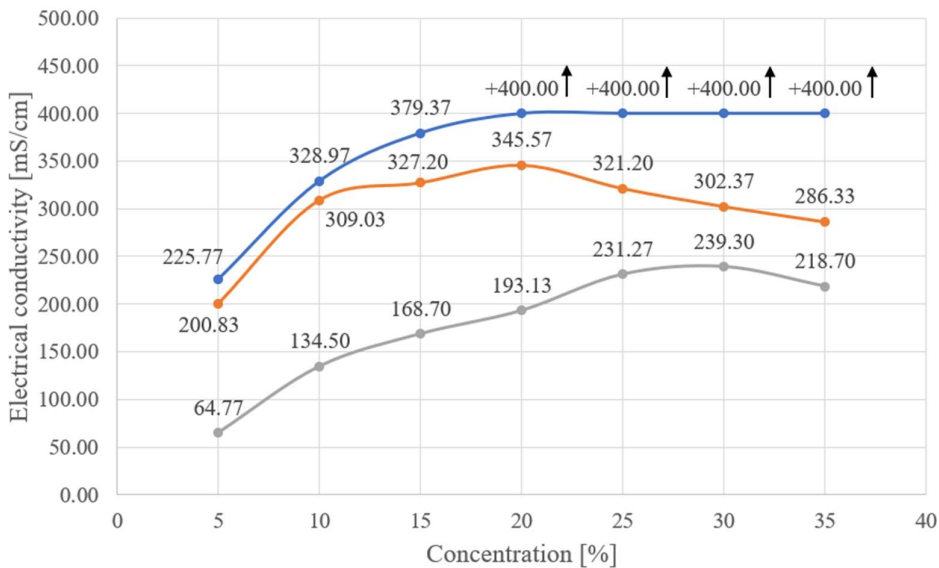


Fig. 14: Electrical conductivity of KOH, NaOH, and NaCl.

**Volumetric flow and mass flow of green hydrogen:** The fixed characteristics for operating the electrolytic cell were determined, such as the voltage and current intensity of the continuous energy source; being 12 V and 18 A, respectively. Furthermore, it is considered that the green hydrogen produced behaves as an ideal gas. Therefore, it is necessary to determine the ambient conditions present to use the ideal gas equation. To calculate the absolute pressure, initially, the height above sea level was determined to be 3250 m, and the environmental temperature was determined using data from the Santa Ana meteorological station located in the city of Huancayo, Junín region - Peru, giving a temperature of 287.15 K, values necessary for equation (14), giving an atmospheric pressure of 0.6813 atm.

The gauge pressure was obtained because the electrolysis process stored the gases in the vessels without leakage, taking into account that the space without electrolyte solution contains air, so the gauge pressure will increase according to the total amount of green hydrogen filling the space; the volume of this space was determined by adding the volume of the cathode region which value is  $220 \text{ cm}^3$ , the volume of the hose which is  $250 \text{ cm}^3$  and the volume of the vessel which is  $289 \text{ cm}^3$ . Thus, the gauge pressure reached an average value of 32 mmHg in the case of green hydrogen, which can be expressed in the same units as atmospheric

pressure as 0.0421 atm. Equation (13) was used to obtain the absolute pressure, which is approximately 0.7214 atm. The molar mass value in the case of hydrogen is  $2 \text{ g}\cdot\text{mol}^{-1}$ , and the temperature was determined with the digital pyrometer (Control Company Traceable 122402526) pointing to the electrolyte solution at the end of each measurement test, where it was observed to be  $31.8^\circ\text{C}$  on average.

In the case of volume, it was calculated through the displacement of water, where the volume of gas produced has a direct relationship to the water displaced, as shown in Fig. 15; furthermore, it is not necessary to fill the space without electrolyte solution with this gas, as the gases expand to fill any space without requiring the gas to occupy the space containing air. Before displacing the water, first, the cell was graduated where the height of the electrolyte solution represents 0 cm. As the electrodes react in the water through electrical energy, the gas produced displaces the water. Consequently, it was determined that in an average of 24 seconds, 0.0475 L of green hydrogen was produced, as shown in Table 8.

A 2.9 L electrolytic solution was prepared for each test in the cell where the temperature, volume, and gauge pressure of the green hydrogen were measured for approximately 24 seconds to determine the volume of the hydrogen, the auxiliary component of oxygen, which consists of a storage

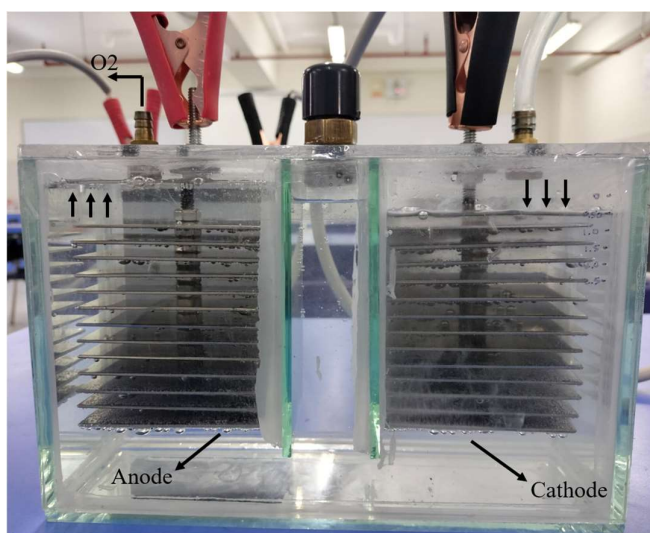


Fig. 15: Water displacement

Table 8: Temperature, Volume, and Pman of green hydrogen.

Repetition	Time [s]	Temperature [K]	Volume [L]	Pman [atm]	Mass [g]
R1	23.7	304.8	0.0475	32	0.002739
R2	24.2	304.9	0.0475	32	0.002738
R3	24.1	304.8	0.0475	32	0.002739

vessel, was removed. Consequently, equation (10) was used to determine the mass of the green hydrogen, resulting in an average of 0.002739 g, as shown in Table 8.

Using these data, the volumetric flow and mass flow of the green hydrogen produced by the electrolytic cell were determined to be  $118.760 \text{ cm}^3 \cdot \text{min}^{-1}$  and  $0.00011 \text{ g} \cdot \text{s}^{-1}$ , respectively. To determine the amount of oxygen produced, the behavior of an ideal gas was taken into account, where it can be inferred that of the total volume of the gas produced, two-thirds is green hydrogen, and one-third is oxygen since one molecule of water is made up of two molecules of hydrogen and one of oxygen, consequently,  $59.380 \text{ cm}^3 \cdot \text{min}^{-1}$  of oxygen is produced as shown in Fig. 16 expressed in  $\text{L} \cdot \text{s}^{-1}$ , which was released into the atmosphere.

To check that the gas produced is green hydrogen, an additional component was assembled to the valve of the

cathodic region, which consists of a bubbler and a Bunsen burner. For this test, the valve of the ignition mechanism was opened and provided with fire; on contact, it was observed that the green hydrogen ignited (Fig. 17), demonstrating that it has a high calorific power and that it can be used to replace conventional fuel.

## DISCUSSION

In the present study, the micro-hydraulic system at most generates 0.055 W and 0.15 A according to the factors studied, which is low in terms of power, unlike other similar turbines (Alonso-Martinez et al. 2020); this is due to the use of an electric generator (DC) with the characteristics specified previously, so it requires 120 hours to charge the continuous energy source with capacity of 18 A per hour, where the charging time is not optimal; however it should

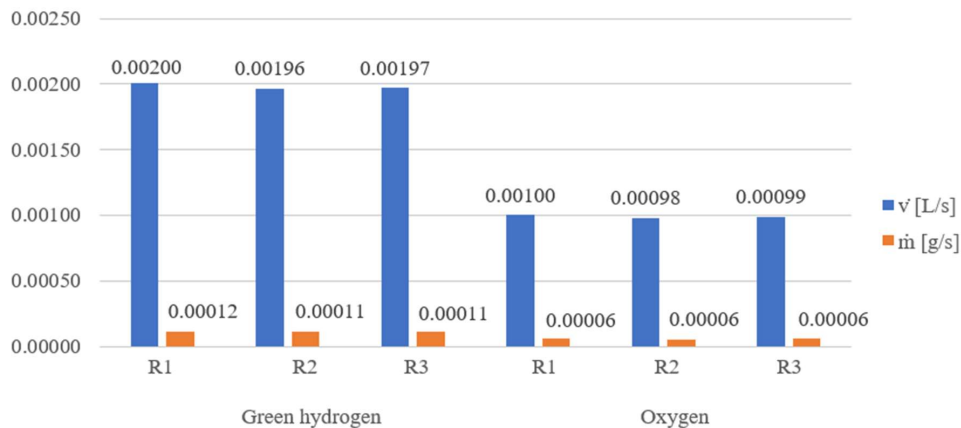


Fig. 16: Volumetric flow ( $\dot{v}$ ) and mass flow ( $\dot{m}$ ) of hydrogen and oxygen.

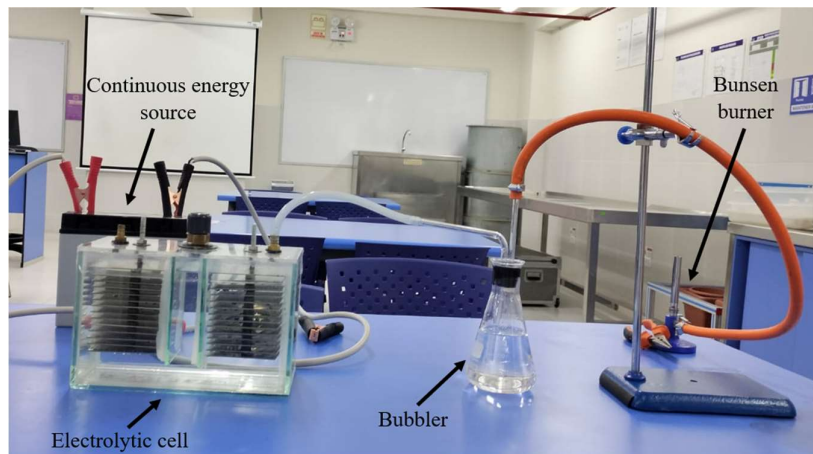


Fig. 17: Ignition test.

be considered to use a suitable electric generator that can minimally support the mechanical potential of the micro-hydraulic system which is 620.25 W. The electrical generator (DC) used does not need a charge controller because it produces a constant flow of energy, unlike an alternating current generator that produces energy with fluctuations, which can damage the continuous energy source.

The electrolytic cell proposed in this study has a higher production rate of green hydrogen than other similar electrolytic cells (Mert et al. 2024, Sanath et al. 2019), being  $118.760 \text{ cm}^3 \cdot \text{min}^{-1}$ , which is since our electrolysis process uses stored energy from the potential energy of water, being the renewable energy resource with the highest operating efficiency compared to other systems that use wind and solar energy, which depend on the environmental conditions where they are located. It should be noted that the micro-hydraulic system can operate all day long; however, when unfavorable meteorological events occur that increase the flow, this system will have to be removed from the body of water where it was placed to avoid possible dragging by the force of the water itself. In addition, the energy generated by the microhydraulic system is stored in a continuous energy source to supply electricity to the electrodes, producing a continuous volumetric flow of green hydrogen, unlike similar electrolytic cells (Mert et al. 2024, Sanath et al. 2019), where the generated energy fluctuates when supplying electricity to their respective electrodes.

Although it is not economically viable to use distilled water, it is preferable to use water from the river where the hybrid system is placed because it is a resource that is found in the environment at no cost. Consequently, it is necessary to determine that the gas produced is green hydrogen without other compounds, carrying out a chromatography analysis, taking into account that within the analysis, nitrogen ( $\text{N}_2$ ) is obtained as one of the components since it is found in the system spaces, as well as other components from the water in case it is residual. To reduce the unwanted components that can be produced from wastewater, it is crucial to adopt measures that are efficient and economical, which must be focused on being implemented in rural areas, considering that these methods are homemade, ecological and environmentally friendly to improve water quality, such as mechanical filtration using sand, gravel and activated carbon filters; coagulation and flocculation using natural substances; and phytoremediation using aquatic plants (Abdiyev et al. 2023, Panday & Ananda Babu 2023).

## CONCLUSIONS

This paper demonstrates the feasibility of a portable hybrid system designed specifically for application in rural areas

with water bodies of low volumetric capacity. The proposed system has been optimized to operate under hydraulic conditions typical of rural environments. The green hydrogen produced by the portable hybrid system can be used as an environmentally friendly fuel due to its high calorific potential, being one of its main characteristics to replace conventional fuel such as LPG which is widely used in rural areas for cooking food. Its potential to change the paradigm of conventional fuel use in isolated communities through a sustainable and cost-effective solution is highlighted.

This work shows that the green hydrogen produced by the portable hybrid system can be used as an ecological fuel due to its high calorific potential, which is one of its main characteristics to substitute the conventional fuel used in rural areas for cooking food, such as LPG; this system uses the energy generated by a microhydraulic system that can be located in water bodies with low volumetric capacity.

In the first stage of the results, it is shown that the wetted area of the water in relation to the Archimedes screw turbine and the fall slope are factors with influence the electric potential, which is contrasted with the rotational speed. Accordingly, it was determined that the micro-hydraulic system, when placed at an angle of elevation equal to  $8.83^\circ$  with a wetted area of 51%, generates a higher electric potential, being 0.055 W. These characteristics can be altered according to the body of water where the microhydraulic system is placed. However, it remains in operation as long as the blades have contact with the water. The influence of slope on the efficiency of hydro turbines is recognized as an established concept; however, our work explores how minor variations in slope can be optimized to maximize micro-hydraulic power production, given that rural areas have low volumetric capacity water bodies such as water channels.

In the second stage, the amount of green hydrogen produced is demonstrated, where the optimal concentration and the appropriate electrolyte to be used in the distilled water is 20% KOH. Also, the continuous energy source is a fixed factor to be considered because it operates with 12 V and 18 A, which influences the amount of green hydrogen produced, which is  $118.760 \text{ cm}^3 \cdot \text{min}^{-1}$ , thus showing a high volumetric flow, considering that the green hydrogen must first be stored in a container to be used later on as a fuel in the cooking of foodstuffs.

Future research is intended to develop the design of a hybrid system with a continuous process to produce green hydrogen more efficiently, maintaining the current advantage of being a portable design and of viable use, where the use of a charge controller should be considered to feed the continuous energy source and at the same time use the electric current in the electrolysis process, in addition to

using a suitable electric generator to take advantage of the capacity of the microhydraulic system and use the water where the hybrid system is placed, as a water resource for the electrolysis process.

## ACKNOWLEDGMENTS

We want to express our sincere thanks to those responsible for the laboratory of the Continental University for their technical support and essential contribution, training us with each piece of equipment used throughout the development of this research.

## NOMENCLATURE

### Symbols

$A_h$	Hydraulic area	[m <sup>2</sup> ]
$A_m$	Wetted area	[%]
$H$	Height above sea level	[m]
$I_c$	Current intensity	[A]
$LT$	Total length of the turbine	[m]
$M$	Mass of the gas	[g]
$\dot{m}$	Mass flow	[g.s <sup>-1</sup> ]
$M$	Molar mass of the gas	[g.mol <sup>-1</sup> ]
$P$	Perimeter	[m]
$P_{abs}$	Absolute pressure	[atm]
$P_{atm}$	Atmospheric pressure	[atm]
$PC$	Fall slope	[°]
$P_e$	Electric potential	[W]
$P_{man}$	Gauge pressure	[atm]
$P_H$	Theoretical potential	[W]
$Q$	Flow rate	[m <sup>3</sup> .s <sup>-1</sup> ]
$R_{he}$	Propeller radius	[m]
$R_h$	Hydraulic radius	[m]
$S$	Slope	[%]
$T$	Time	[s]
$T$	Torque	[Nm]
$T_c$	Electrolytic cell temperature	[K]
$T_g$	Environmental temperature	[K]
$V$	Volume of green hydrogen	[L]
$\dot{v}$	Volumetric flow	[L.s <sup>-1</sup> ]
$V_f$	Flow velocity	[m.s <sup>-1</sup> ]
$Volt$	Voltage	[V]
$W$	Angular velocity	[rad.s <sup>-1</sup> ]

$Y_c$  Propeller inertia [m]

### Greek letters

$P$	Density	[kg.m <sup>-3</sup> ]
$A$	Inclination angle of propellers	[°]
$\Theta$	Inclination angle of the turbine	[°]

### Subscripts and superscripts

Int	Internal PC Y Am
CH <sub>4</sub>	Methane
CO	Carbon monoxide
CO <sub>2</sub>	Carbon dioxide
H <sub>2</sub>	Hydrogen
N <sub>2</sub>	Nitrogen
N <sub>2</sub> O	Nitrous oxide
O <sub>2</sub>	Oxygen

### Abbreviations

IEA	International Energy Agency
DC	Direct Current
IPCC	Intergovernmental Panel on Climate Change
LPG	Liquefied Petroleum Gas
RPM	Revolutions Per Minute
WHO	World Health Organization

## REFERENCES

- Abdiyev, K., Azat, S., Kuldeyev, E., Ybyraimkul, D., Kabdrakhmanova, S., Berndtsson, R., Khalkhabai, B., Kabdrakhmanova, A. and Sultakhan, S., 2023. Review of slow sand filtration for raw water treatment with potential application in less-developed countries. *Water (Switzerland)*, 15, p.11207. [DOI]
- Albornoz, M., Rivera, M., Wheeler, P. and Ramírez, R., 2023. High pulsed voltage alkaline electrolysis for water splitting. *Sensors*, 23, p.820. [DOI]
- Alonso-Martinez, M., Sierra, J.L.S., Díaz, J.J.D.C. and Martinez-Martinez, J.E., 2020. A new methodology to design sustainable Archimedean screw turbines as green energy generators. *International Journal of Environmental Research and Public Health*, 17, p.236. [DOI]
- Babay, M.A., Adar, M., Chebak, A. and Mabrouki, M., 2023. Dynamics of gas generation in porous electrode alkaline electrolysis cells: An investigation and optimization using machine learning. *Energies (Basel)*, 16. [DOI]
- Bideau, D., Chocron, O., Mandin, P., Kiener, P., Benbouzid, M., Sellier, M., Kim, M., Ganci, F. and Inguanta, R., 2020. Evolutionary design optimization of an alkaline water electrolysis cell for hydrogen production. *Applied Sciences (Switzerland)*, 10, pp.614-625. [DOI]
- Cao, X., Wang, J., Zhao, P., Xia, H., Li, Y., Sun, L. and He, W., 2023. Hydrogen production system using alkaline water electrolysis adapting to fast fluctuating photovoltaic power. *Energies (Basel)*, 16, pp.23-41. [DOI]

- Chen, H., Gu, S., Jia, C., Gu, H., Xu, Q. and Lin, Z., 2023. Effects of household clean fuel combustion on the physical and mental health of the elderly in rural China. *Sustainability (Switzerland)*, 15, pp.61-78. [DOI]
- Colli, A.N., Girault, H.H. and Battistel, A., 2019. Non-precious electrodes for practical alkaline water electrolysis. *Materials*, 12, p.813. [DOI]
- Díaz-Salas, A., Guevara-Pérez, E. and Rosales-Cueva, J., 2020. Estimation model of the Manning roughness coefficient as a function of granulometry in the Santa River, Recuay-Carhuaz sector, Ancash, Perú. *Revista Ingeniería UC*, 27, pp.328-342. [DOI]
- Dragomirescu, A., 2021. Design considerations for an Archimedean screw hydro turbine. *IOP Conference Series: Earth and Environmental Science*, 11, pp.491-513. [DOI]
- Elgarahy, A.M., Eloffy, M.G., Hammad, A., Saber, A.N., El-Sherif, D.M., Mohsen, A., Abouzid, M. and Elwakeel, K.Z., 2022. Hydrogen production from wastewater, storage, economy, governance and applications: A review. *Environmental Chemistry Letters*, 20, pp.3453-3504. [DOI]
- Fathi, E., Arcentales, D. and Belyadi, F., 2023. Impacts of different operation conditions and geological formation characteristics on CO<sub>2</sub> sequestration in Citronelle Dome, Alabama. *Energies (Basel)*, 16, p.713. [DOI]
- Fersch, B., Wagner, A., Kamm, B., Shehaj, E., Schenk, A., Yuan, P., Geiger, A., Moeller, G., Heck, B., Hinz, S., Kutterer, H. and Kunstmann, H., 2022. Tropospheric water vapor: A comprehensive high-resolution data collection for the transnational Upper Rhine Graben region. *Earth System Science Data*, 14, pp.5287-5307. [DOI]
- Gavrailov, D.Y. and Boycheva, S.V., 2023. Study assessment of water electrolysis systems for green production of pure hydrogen and natural gas blending. *IOP Conference Series: Earth and Environmental Science*, 41(9), pp.234-246. [DOI]
- Hamidah, I., Solehudin, A., Setiawan, A., Hasanah, L., Mulyanti, B., Nandiyanto, A.B.D. and Khairurrijal, K., 2018. Surface of AISI 316 as electrode material for water electrolysis under potassium hydroxide for hybrid car application. *International Journal of Automotive and Mechanical Engineering*, 15, pp.5863-5873. [DOI]
- Hassan, Q., Abbas, M. K., Tabar, V. S., Tohidi, S., Abdulrahman, I. S. and Salman, H. M., 2023. Sizing electrolyzer capacity in conjunction with an off-grid photovoltaic system for the highest hydrogen production. *Energy Harvesting and Systems*, 10(4), pp.331-348. [DOI]
- Islam, A., Sarkar, B., Saha, U. D., Islam, M. and Ghosh, S., 2022. Can an annual flood induce changes in channel geomorphology? *Natural Hazards*, 111, pp.1019-1046. [DOI]
- Marouani, I., Guesmi, T., Alshammari, B. M., Alqunun, K., Alzamil, A., Alturki, M. and Hadj Abdallah, H., 2023. Integration of renewable-energy-based green hydrogen into the energy future. *Processes*, 11(9), pp. [DOI]
- Mert, M. E., Edis, C., Akyıldız, S., Demir, B. N., Nazligül, H., Gurdal, Y. and Doğru Mert, B., 2024. Design and performance analysis of PV-assisted alkaline electrolysis for hydrogen production: An experimental and theoretical study. *Fuel*, 355, p.129497. [DOI]
- Muhsen, H., Al-Mahmodi, M., Tarawneh, R., Alkhraibat, A. and Al-Halhoul, A., 2023. The potential of green hydrogen and power-to-X utilization in Jordanian industries: Opportunities and future prospects. *Energies*, 17(1), pp. [DOI]
- Muñoz-Maldonado, Y., Correa-Quintana, E. and Ospino-Castro, A., 2023. Electrification of industrial processes as an alternative to replace conventional thermal power sources. *Energies*, 16(19), pp. [DOI]
- Nasser, M., Megahed, T. F., Ookawara, S. and Hassan, H., 2022. A review of water electrolysis-based systems for hydrogen production using hybrid/solar/wind energy systems. *Environmental Science and Pollution Research*, 29, pp.86994-87018. [DOI]
- Niroula, S., Chaudhary, C., Subedi, A. and Thapa, B. S., 2023. Parametric modeling and optimization of alkaline electrolyzer for the production of green hydrogen. *IOP Conference Series: Materials Science and Engineering*, 1279(1), p.012005. [DOI]
- Osman, A. I., Mehta, N., Elgarahy, A. M., Hefny, M., Al-Hinai, A., Al-Muhtaseb, A. H. and Rooney, D. W., 2022. Hydrogen production, storage, utilisation and environmental impacts: A review. *Environmental Chemistry Letters*, 20, pp.153-188. [DOI]
- Panday, V. and Ananda Babu, K., 2023. The potential of phytoremediation to treat different types of wastewater: A review. *Nature Environment and Pollution Technology*, 22(2), pp.969-975. [DOI]
- Sanath, Y., De Silva, K., Middleton, P. H. and Kolhe, M., 2019. Performance analysis of single-cell alkaline electrolyzer using a mathematical model. *IOP Conference Series: Materials Science and Engineering*, 605(1), p.012002. [DOI]
- Sánchez, A. C., Galeano, W. F. and Zambrano, J. M., 2023. Design of a micro-hydraulic generation system based on an Archimedes screw. *Ingenius*, 29, pp.98-107. [DOI]
- Song, H., Kim, Y. and Yang, H., 2023. Design and optimization of an alkaline electrolysis system for small-scale hydropower integration. *Energies*, 17, pp. [DOI]
- Yakubson, K. I., 2022. Prospects for using hydrogen in various branches of the world economy as one of the directions of its decarbonization. *Russian Journal of Applied Chemistry*, 95, pp.309-340. [DOI]
- Zhang, L., Jia, C., Bai, F., Wang, W., An, S., Zhao, K., Li, Z., Li, J. and Sun, H., 2024. A comprehensive review of the promising clean energy carrier: Hydrogen production, transportation, storage, and utilization (HPTSU) technologies. *Fuel*, 355, p.129455. [DOI]